RF Technology Optimization by a Fast Method for Linearity Determination

T. V. Dinh[a], A. Vohra[b], J. Melai[b], T. Vanhoucke[a], P. H. C. Magnee[b] and D. B. M. Klaassen[c]

[a] NXP Semiconductors Leuven, Interleuvenlaan 80, 3001 Leuven, Belgium;
[b] NXP Semiconductors Nijmegen, Gerstweg 2, 6534 AE Nijmegen, The Netherlands;
[c] NXP Semiconductors Eindhoven, High-Tech Campus 46, 5656 AE Eindhoven, The Netherlands.

***Abstract*—This paper introduces a new methodology to determine the small signal linearity of a device directly from 2-port Y-parameters. With that approach, a 10-fold reduction of the simulation time in a comparison with traditional transient or harmonic balance simulations can be achieved, which enables a fast route for RF device and process technology optimization in an industrial environment. It is also shown that the linearity performance should be taken into account for the device optimization.**

***Keywords*—Linearity; RF; device; process; TCAD; SiGe HBT; 2-port; Y-parameters**

I. Introduction

Process and device simulation (TCAD) have been widely used to optimize RF devices and technologies. Optimization is often based on traditional figures of merit (FOM) which can be obtained directly from TCAD, including DC (*I-V* curves) and small-signal RF quantities (e.g. capacitances, cutoff frequency f_T, maximum-oscillation frequency f_{MAX}). For sophisticated RF applications two other aspects need special attention: noise and linearity. Fast and efficient methodologies have been introduced for RF noise prediction, either directly from TCAD e.g. [1-4] or from DC measurements [5]. However, only few studies on linearity have been published. High-frequency linearity is a measure of the level of generated higher harmonics which distort the signal at the fundamental frequency. One of the most important figures of merits for small-signal linearity is the input and output third-order intercept point (IIP3 and OIP3) – which is obtained by extrapolating the power of the fundamental and third harmonic by a theoretical small-signal slope. With TCAD, linearity can be evaluated by transient simulations which is very time

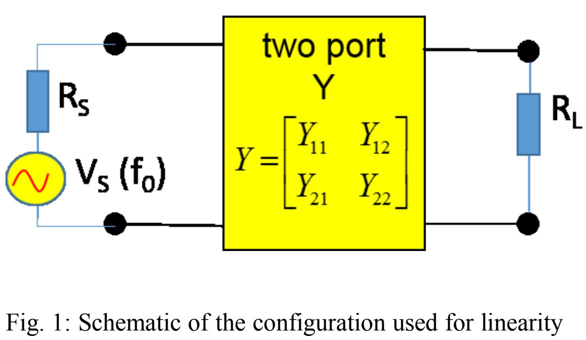

Fig. 1: Schematic of the configuration used for linearity determination (R_S=R_L=50Ω, f_0=5GHz).

consuming [6-8] or by harmonic-balance (HB) simulation where there are often problems with the simulation convergence [9-12]. Therefore, in the literature Volterra series expansions have been commonly used for this purpose e.g. [13-14]. However, with this approach, (compact) model expressions have to be assumed in order to introduce nonlinearities and it does not lead to an explicit relation of the linearity with Y-parameters. In this paper, we present a new, fast method for determining the small-signal linearity of a 2-port directly from simulated or measured Y-parameters without any prior knowledge of the device. This method yields a reduction of the simulation time of about a factor of 10 compared to conventional TCAD HB simulations [12]. Since the linearity performance is shown to be necessary in any device optimization, this fast method can be integrated into the existing platform to become a viable and efficient optimization tool for RF technology.

II. Methodology

A. Approach

Assuming that *i*) all excitations are in the small-signal regime and that *ii*) all capacitances are frequency-independent, the voltages υ and currents i at frequency f_0 (fundamental frequency), $2f_0$ and $3f_0$ can be expressed in terms of the higher-order derivatives of the 2-port Y-parameters, e.g.

$$i_{1,3f_0} = Y_{11}^{3f_0} \cdot \upsilon_{1,3f_0} + Y_{12}^{3f_0} \cdot \upsilon_{2,3f_0} + i_{1,3f_0,gen}, \tag{1}$$

and a similar expression for $i_{2,3f_0}$. "$3f_0$" indicates the frequency and $i_{1,3f_0,gen}$ stands for the current generated at the input and at $3f_0$ due to mixing of signals at f_0 and $2f_0$ as

$$\begin{aligned} i_{1,3f_0,gen} = {} & C_1 \cdot \upsilon_{1,f_0} \cdot \upsilon_{1,2f_0} + C_2 \cdot \upsilon_{1,f_0} \cdot \upsilon_{2,2f_0} + C_3 \cdot \upsilon_{1,2f_0} \cdot \upsilon_{2,f_0} + \\ & C_4 \cdot \upsilon_{2,f_0} \cdot \upsilon_{2,2f_0} + C_5 \cdot \upsilon_{1,f_0}^3 + C_6 \cdot \upsilon_{1,f_0}^2 \cdot \upsilon_{2,f_0} + \\ & C_7 \cdot \upsilon_{1,f_0} \cdot \upsilon_{2,f_0}^2 + C_8 \cdot \upsilon_{2,f_0}^3 \end{aligned} \tag{2}$$

The coefficients C_k can be expressed in terms of (higher order) derivatives of the Y-parameters while those derivatives can be obtained by using close neighboring bias points. The relation between the currents and the voltages at in- and output is determined by the source and load impedance, respectively.

978-1-4673-7860-4/15/$31.00 ©2015 IEEE

Similarly, the currents at $2f_0$ are obtained from

$$i_{1,2f_0} = Y_{11}^{2f_0} \cdot \upsilon_{1,2f_0} + Y_{12}^{2f_0} \cdot \upsilon_{2,2f_0} + i_{1,2f_0,gen}, \tag{3}$$

and a similar expression for $i_{2,2f_0}$. Again $i_{1,2f_0,gen}$ stands for the current generated at the input and at $2f_0$ due to mixing of signals at f_0, which is

$$i_{1,2f_0,gen} = C_9 \cdot \upsilon_{1,f_0}^2 + C_{10} \cdot \upsilon_{1,f_0} \cdot \upsilon_{2,f_0} + C_{11} \cdot \upsilon_{2,f_0}^2 \tag{4}$$

From (1) – (4), voltages and currents at various harmonics at the input and output of the 2-port can be derived, hence the power of different harmonics can be calculated.

B. Validation

The methodology is applied to state-of-the-art high voltage SiGe HBT devices having an f_T above 40GHz [15]. As the fundamental frequency f_0 is 5GHz, the assumption of frequency-independent capacitances is valid. After Y parameters at different bias points (V_{CE} and V_{BE}) are generated from device simulations, they are fed directly into the linearity calculator developed in this work to obtain the power of harmonics at those biases. Then the results are validated against harmonic balance simulations done at those conditions.

The full setup of the HB simulations is similar to the work presented in [11]. At the input, a one-tone voltage source with the fundamental frequency f_0 and small voltage swing, connected with a resistor of 50Ω is chosen. At the output, a load of 50Ω is used. Bias tees to separate the DC bias and RF signal at in- and output are applied. Fig. 2 shows the fundamental, the second and the third harmonics obtained from HB simulations and the new methodology for V_{BE} from 0.6V

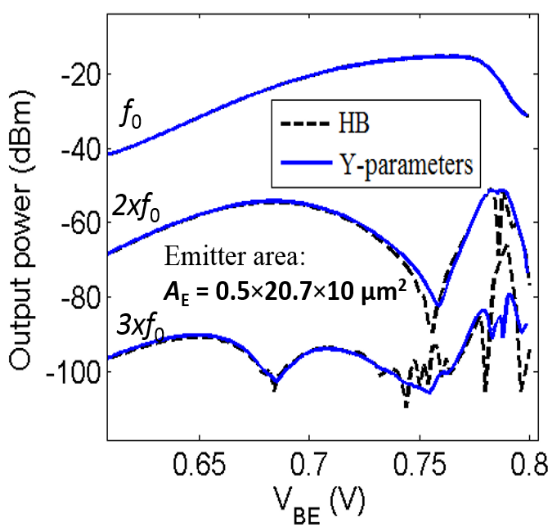

Fig. 2: Comparison of the output power at harmonics obtained from harmonic balance (HB) simulation and calculation from Y-parameters (SiGe HBT with BV_{CEO} of 4.0V, f_T of 40GHz, V_{CE}=2V; see Fig. 4).

to 0.8V (i.e. from the ideal region to the region beyond peak f_T, see Fig. 4). An excellent agreement between these two types of simulations has been obtained.

Another advantage of the new methodology is that it facilitates a sensitivity analysis to assess the dominant contributions to the non-linearity. One example is shown in Fig. 3. Here most important components (noted as C), which accounts for most of the distortion in the device, are analyzed. The sensitivity is defined as the change in the power of the third harmonic in response to a change in one of those components. It is seen that the contribution of each component varies over the bias, e.g. at low V_{BE}, $\frac{d^2}{dV_1^2}\mathrm{Re}(Y_{21})$ and $\frac{d}{dV_1}\mathrm{Re}(Y_{21})$ are the most important to the linearity while at higher V_{BE} (near peak f_T) other components (e.g. $\frac{d}{dV_1}\mathrm{Im}(Y_{21})$ and $\frac{d}{dV_1}\mathrm{Im}(Y_{11})$)

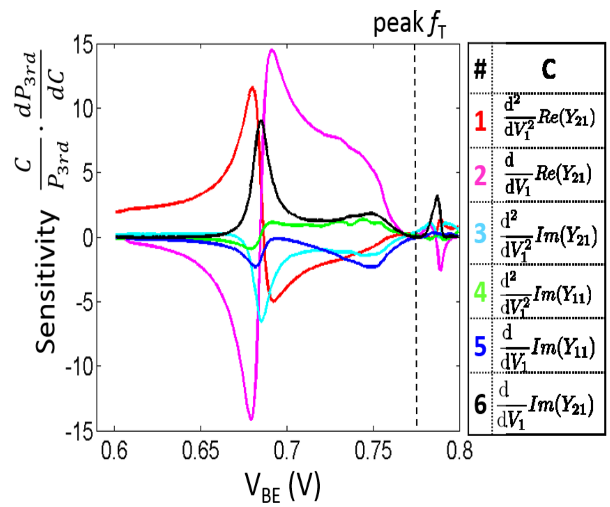

Fig. 3: Sensitivity analysis of the third harmonic power P_{3rd} in response to the six most important components (SiGe HBT with BV_{CEO} of 4.0V, f_T of 40GHz, V_{CE}=2V; see Fig. 4).

become more significant. By visualizing the impact of each component to the distortion in this way, an insight into the device linearity can be understood which helps for the device and process optimization.

It is worth mentioning again that this methodology can be applied to any type of device as long as a 2-port configuration can be setup to obtain Y-parameters (either from measurements or simulations) as shown in the schematic from Fig. 1.

C. Application to measurements

Next the methodology is applied to measurements and compared to simulations using a well-calibrated TCAD deck. The Gummel plots (base and collector currents), f_T and f_{MAX} obtained from TCAD match very well with the measurements, which are shown in Fig. 4. Also a good matching has been observed for all Y parameters (which are not shown here). This agreement is a prerequisite for any further comparison at the harmonic power level.

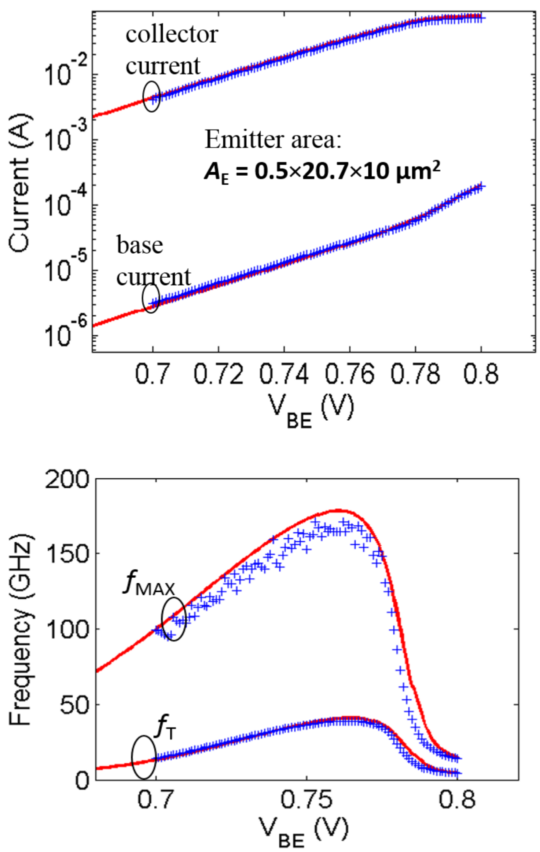

Fig. 4: DC and RF performance from TCAD (line) and measurement (symbol) for the SiGe HBT (referred in this work as the reference device) at V_{CE}=2V.

Fig. 5 shows the output powers and OIP3 obtained from our new methodology, with the input either from measured Y-parameters or from simulated (TCAD) Y-parameters. Very good agreement is achieved up to the second-order harmonics. However, for the third harmonic, there is a small difference, which might be due to imperfections in the higher-order derivatives of the physical TCAD models. This should be studied in more detail, but such a study is beyond the scope of this work. For now it suffices to note that the HB method does not yield greater accuracy (cf. Fig. 2).

III. Technology Optimization

The new methodology has been used to optimize the RF device and process. Again, the SiGe HBT with the electrical characteristics in Fig. 4 is chosen as the reference device for further optimization. Since the collector profile determines some of the most important characteristics of the HBT device which have an impact on the RF linearity (e.g. [7-8]) including the breakdown voltage, f_T roll-off and collector base capacitance (i.e. $Im(Y_{21})$ as shown in Fig. 3), it is chosen to be optimized in this work. The base and emitter are kept unchanged.

In the first optimization approach, the collector profile of

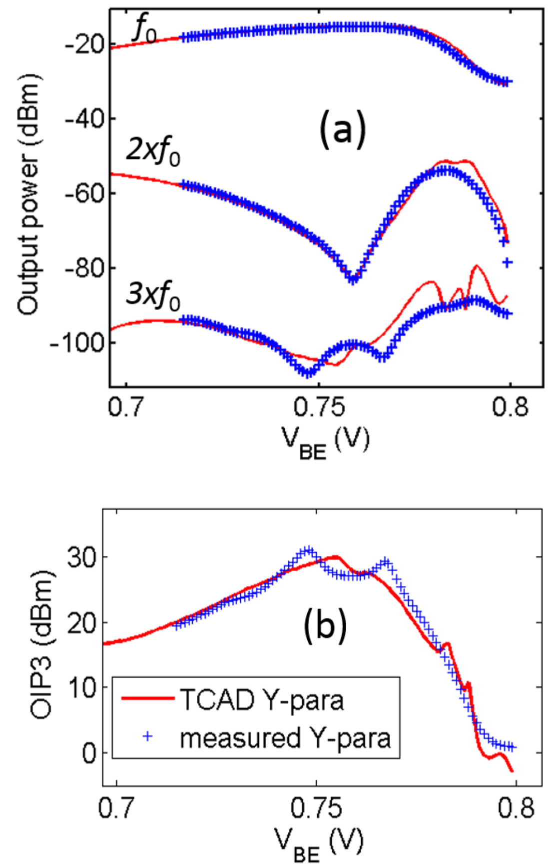

Fig. 5: (a) The output power at harmonics and (b) OIP3 calculated with the input of Y-parameters either from TCAD or from measurement at V_{CE}=2.

the new device is made to be flatter and shorter than that of the reference device in the condition that both of them have similar breakdown voltages (BV_{CEO} of ~ 4V, and BV_{CBO} of ~ 17V). The device with this profile is called device 1. A higher f_T is expected for device 1 (compared to the reference device) due to its lower collector series resistance. In the second optimization, a much steeper and higher dope for the collector profile is chosen. This type of profile is called device 2. The breakdown voltages of device 2 is lower than those of other two devices (BV_{CEO} of ~3V and BV_{CBO} of 15V).

Results for f_T, IIP3 and OIP3 of these devices are shown in Fig. 6. Due to a higher dope in the collector, device 2 can delay the onset of Kirk-effect, which in turn has a higher peak f_T. As a result, it is also delivering the highest linearity at higher V_{BE} (or higher collector current density). However, it is more complicated to make a comparison of the performance between device 1 and the reference device. Although device 1 has a slightly better f_T, its linearity is slightly smaller than the reference device. Therefore, from this figure it can be seen that optimizing for f_T may lead to different results than optimizing for linearity. This illustrates that the linearity performance should be taken into account for RF device and process optimization.

IV. Conclusion

A new, fast methodology to evaluate the small-signal linearity performance of 2-ports has been introduced and validated on simulations and measurements. Applying this methodology to SiGe HBT technology optimization, it has been shown that it is essential to include the linearity performance in this optimization.

Acknowledgment

We would like to acknowledge Jan Slotboom, Anco Heringa, Fred Hurkx, Erwin Hijzen, Mark van der Heijden, and Domine Leenaerts for valuable discussions, and the whole BiCMOS team in Nijmegen for processing all these devices.

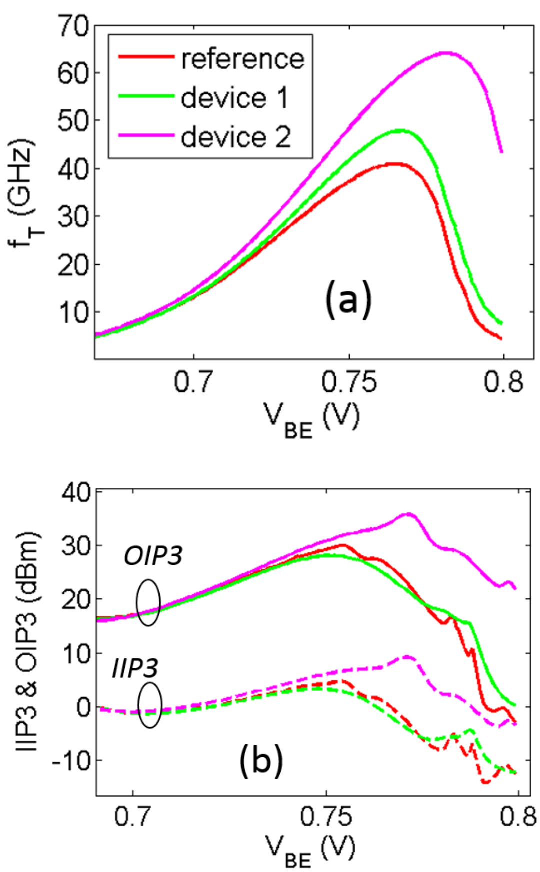

Fig. 6: f_T and IIP3/OIP3 of the optimized devices compared with the reference device (device 1: flatter collector profile and a higher sub-collector dope for a lower series resistance; device 2: steeper profile with a higher collector dope) at V_{CE}=2V.

References

[1] C. M. van Vliet, "Macroscopic and microscopic methods for noise in devices", IEEE Trans. Electron Devices, vol. 41, pp. 1902-1915, 1994.

[2] G. Bonani, G. Ghione, M. R. Pinto, and R. K. Smith, "An efficient approach to noise analysis through multidimensional physics-based models", IEEE Trans. Electron Device, vol. 41, no. 1, pp. 261-269, 1998

[3] C. Jungemann, B. Neinhus, B. Meinerzhagen, and R. W. Dutton, "Investigation of compact models for RF noise in SiGe HBTs by Hydrodynamic device simulation", IEEE Trans. Electron Devices, vol. 51, pp. 956-961, 2004.

[4] T. Vanhoucke, D. B. M. Klaassen, H. Mertens, J. J. T. M. Donkers, G. A. M. Hurkx, H. G. A. Huizing, P. H. C. Magnee, E. A. Hijzen, R. van Dalen, E. Gridelet, and J. W. Slotboom, "Virtual technology for RF process and device development", IEEE BCTM Proceedings, pp. 37-44, 2011.

[5] E. Gridelet, A. J. Scholten, D. B. M. Klaassen, R. van Dalen, R. Pijper, P. H. C. Magnee, L. F. Tiemeijer, T. V. Dinh, and T. Vanhoucke, "Fast noise prediction for process optimization by using only standard DC and S-parameters measurements", IEEE BCTM Proceedings, pp. 104-107, 2012.

[6] L. C. N. de Vreede, H. C. de Graaff, J. A. Willemen, W. D. van Noort, R. Jos, L. E. Larson, J. W. Slotboom, J. L. Tauritz, "Bipolar transistor epilayer design using the MAIDS mixed-level simulator", IEEE Journal of Solid State Circuits, Vol.34, pp.1331-1338, 1999.

[7] W. D. van Noort, L. C. N. de Vreede, H. F. F. Jos, L. K. Nanver, J. W. Slotboom, "Reduction of UHF power transistor distortion with a nonuniform collector doping profile", IEEE Journal of Solid State Circuits, Vol.36, pp.1399-1405, 2001.

[8] B. G. Malm and M. Östling, "Mixed mode circuit and device simulation of RF harmonic distortion for high-speed SiGe HBTs", Solid State Electronics, vol. 46, pp. 1567-1571, 2002.

[9] B. Troyanovsky, Z. Yu, L. So, and R. W. Dutton, "Relaxation-based harmonic balance technique for semiconductor device simulation", ICCAD, pp.700-703, 1995.

[10] Z. Yu, R. W. Dutton, B. Troyanovsky, and J. Sato-Iwanaga, "Large signal analysis of RF circuits in device simulation", IEICE Trans. Electron, vol. E82-C, no. 6, pp.908-916, 1999.

[11] T. V. Dinh, R. Pijper, T. Vanhoucke, E. Gridelet, and D. B. M. Klaassen, "Investigation of power and linearity performance for low- and high-voltage SiGe HBTs", IEEE BCTM Proceedings, pp. 9-12, 2013.

[12] Synopsys Sentaurus Process and Device Simulation, 2014.

[13] M. Schröter, D. R. Pehlke, and Tzung-Yin Lee, "Compact modeling of high-frequency distortion in silicon integrated bipolar transistors", IEEE Trans. Electron Device, vol. 47, no. 7, pp.1529-1535, 2000.

[14] G. Niu, Q. Liang, J. D. Cressler, C. S. Webster, "RF linearity characteristics of SiGe HBTs", IEEE Trans. Microwave Theory & Technique, vol. 49, no. 9, pp. 1558-1565, 2001.

[15] H. Mertens, P. H. C. Magnee, J. J. T. M. Donkers, E. Gridelet, P. Huiskamp, D. B. M. Klaassen, and T. Vanhoucke, "Extended high voltage HBTs in a high-performance BiCMOS process", IEEE BCTM Proceedings, pp. 158-161, 2011.